

# Evidence for a Spatially-Modulated Superfluid Phase of $^3\text{He}$ under Confinement

Lev V. Levitin,<sup>\*</sup> Ben Yager,<sup>†</sup> Laura Sumner,<sup>‡</sup> Brian Cowan, Andrew J. Casey, and John Saunders  
*Department of Physics, Royal Holloway University of London, Egham, Surrey, TW20 0EX, UK*

Nikolay Zhelev,<sup>§</sup> Robert G. Bennett,<sup>¶</sup> and Jeevak M. Parpia  
*Department of Physics, Cornell University, Ithaca, NY, 14853 USA*  
(Dated: 15 January 2019)

In superfluid  $^3\text{He}$ -B confined in a slab geometry, domain walls between regions of different order parameter orientation are predicted to be energetically stable. Formation of the spatially-modulated superfluid *stripe phase* has been proposed. We confined  $^3\text{He}$  in a  $1.1\ \mu\text{m}$  high microfluidic cavity and cooled it into the B phase at low pressure, where the stripe phase is predicted. We measured the surface-induced order parameter distortion with NMR, sensitive to the formation of domains. The results rule out the stripe phase, but are consistent with 2D modulated superfluid order.

PACS numbers: 67.30.H-, 67.30.hr, 67.30.hj, 74.20.Rp

The pairing of fermions to form a superfluid or superconductor at sufficiently low temperatures is a relatively ubiquitous phenomenon [1, 2]. Examples include: electrically conducting systems from metals to organic materials to metallic oxides [3]; neutral atoms from  $^3\text{He}$  [4, 5] to ultracold fermionic gases [6]; and astrophysical objects such as neutron stars and pulsars [7]. In the most straightforward case the pairs form a macroscopic quantum condensate which is spatially uniform. In type-II superconductors a spatially inhomogeneous state, the Abrikosov flux lattice, arises in a magnetic field [8]. Its origin is the negative surface energy between normal and superconducting regions. However the realisation and experimental identification of states with spatially-modulated superfluid/superconducting order has proved challenging.

The Fulde-Ferrell-Larkin-Ovchinnikov (FFLO) state [9, 10], has been predicted to arise in *spin-singlet* superconductors. An imbalance between spin-up and spin-down Fermi momenta, driven by ferromagnetic interactions or high magnetic fields, induces pairing with non-zero centre of mass momentum. This results in both the order parameter and the spin density oscillating in space with the same wavevector. The FFLO state is predicted to intervene beyond the Pauli limiting field, inhibiting the destruction of superconductivity [11]. It requires orbital effects to be weak, restricting possible materials for its observation. There is evidence of the FFLO state in the layered organic superconductors  $\kappa$ -(BEDT-TTF) $_2\text{Cu}(\text{NCS})_2$  and  $\beta''$ -(ET) $_2\text{SF}_5\text{CH}_2\text{CF}_2\text{SO}_3$  [12–16], and in the canonical heavy fermion superconductor  $\text{CeCu}_2\text{Si}_2$  [17]. Previously identified as FFLO [18], a more complex state, with intertwined p-wave pair density wave (PDW) and spin density wave has been proposed in the heavy fermion d-wave superconductor  $\text{CeCoIn}_5$  [19–21]. Elsewhere a PDW commensurate with a charge density wave, has been clearly demonstrated in the d-wave cuprate superconductor  $\text{Bi}_2\text{Sr}_2\text{CaCu}_2\text{O}_{8+x}$  [22]. In the ultracold fermionic gas  $^6\text{Li}$ , superfluidity with im-

balanced spin populations has been observed [23] with thermodynamic evidence consistent with FFLO [24]. In addition to these condensed matter systems it has been proposed that quantum chromodynamics may provide a pathway to inhomogeneous superconductivity, potentially realised in astrophysical objects [25].

In general the order parameter modulation is expected to be more complex than the model FFLO state [11, 26]. Potential examples are: 1D domain walls of thickness much smaller than the width of domains; 2D modulated structures, involving multiple wavevectors [11]. Furthermore, nucleation barriers and metastability may inhibit the formation of periodic states [26].

In this paper we report experimental investigation of a predicted spatially modulated state in the topological p-wave, *spin-triplet*, superfluid  $^3\text{He}$  [27]. This requires the superfluid to be confined in a thin cavity of uniform thickness. At the heart of this predicted *stripe phase* is the stabilisation of a hard domain wall, of thickness comparable to the superfluid coherence length, in superfluid  $^3\text{He}$ -B under confinement in a slab geometry. These B-B domain walls were first classified in Ref. [28], and the analogy drawn with cosmic domain walls. Their stability in the bulk, and possible evidence for their observation is discussed in [29]. Under confinement the presence of the domain wall reduces surface pair-breaking, and can result in a negative domain wall energy, leading to the formation of the stripe phase [27, 30, 31].

In superfluid  $^3\text{He}$  the nuclear spins constitute the spin part of the pair wavefunction; thus nuclear magnetic resonance (NMR) is widely used to provide a direct fingerprint of the superfluid order parameter [4, 5]. NMR has been predicted to distinguish clearly between the striped and translationally-invariant states of the B phase [30, 32].

To optimise the formation of stripes in this work we chose a slab geometry of height  $D = 1.1\ \mu\text{m}$ , where the B phase is stable down to zero pressure [33]. The stripe phase was originally predicted in the weak-coupling

limit of Bardeen-Cooper-Schrieffer theory [27], while the strong-coupling corrections to this theory in general favour the A phase and suppress the stability of stripes [30]. At present the strong coupling effects are not fully understood theoretically, leaving the stability of the stripe phase an open question [30, 33]. We performed the experiment at low pressure to minimise the strong-coupling effects.

Here we show that under our experimental conditions the stripe phase is clearly ruled out. However, there is NMR evidence for a spatially modulated superfluid of two-dimensional morphology, similar to states discussed in the context of FFLO [11]; we term this *polka-dot*.

The  $3 \times 3$  matrix order parameter of a p-wave superfluid  ${}^3\text{He}$  allows for multiple superfluid phases with different broken symmetries and topological invariants [4, 5]. In the bulk, at low pressure and magnetic field the stable state is the quasi-isotropic B phase with order parameter matrix  $\mathbf{A} = e^{i\phi} \mathbf{R} \Delta$ , where  $\Delta$  is the energy gap, isotropic in the momentum space,  $\phi$  is the superfluid phase and  $\mathbf{R} = \mathbf{R}(\hat{\mathbf{n}}, \theta)$  is the matrix of relative spin-orbit rotation, parametrised by angle  $\theta$  and axis  $\hat{\mathbf{n}}$ . This quasi-isotropic phase is relatively easily distorted by magnetic field or flow. Under confinement the distortion is strong and spatially inhomogeneous, induced by surface pair-breaking. In a slab normal to the  $z$ -axis, the order parameter is predicted to take the form

$$\mathbf{A}(z) = e^{i\phi} \mathbf{R} \begin{pmatrix} \Delta_{\parallel}(z) & & \\ & \Delta_{\parallel}(z) & \\ & & \Delta_{\perp}(z) \end{pmatrix}, \quad (1)$$

with  $0 \leq \Delta_{\perp} < \Delta_{\parallel}$  due to stronger surface pair-breaking of Cooper pairs with orbital momentum parallel to the slab surface [34]. This distortion is named *planar* after the planar phase, in which  $\Delta_{\perp} = 0$  [5].

The order parameter (1) has a large manifold of orientations, determined by  $\phi$ ,  $\hat{\mathbf{n}}$  and  $\theta$ , allowing domain walls between regions of different orientations [28, 29]. Domain walls where  $\Delta_{\perp}$  changes sign, shown in Fig. 1, are predicted to have negative surface energy in the B phase confined in a thin slab, close to the A-B transition [27, 35]. As a consequence the slab of  ${}^3\text{He-B}$  would spontaneously break into domains, until the domain walls get close enough that their mutual repulsion becomes significant. This is predicted to result in the periodic stripe phase with a typical domain size  $W$  of order  $D$  [27, 30, 31]. Phases with spontaneously broken translational invariance are also predicted to stabilise in  ${}^3\text{He}$  confined to narrow pores [36, 37] and in films of d-wave superconductors [38].

In this experiment we performed pulsed NMR studies on a slab of  ${}^3\text{He}$  confined in a  $D = 1144 \pm 7$  nm thick silicon-glass microfluidic cavity, in a field of 31 mT perpendicular to the slab (corresponding to  ${}^3\text{He}$  Larmor frequency  $f_L = 1.02$  MHz), using the setup described in Refs. [39, 40]. The measurements were performed at low

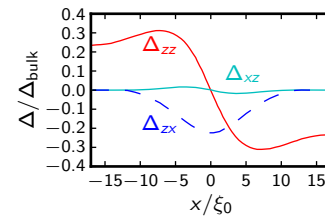


FIG. 1. Domain wall at the heart of the stripe phase in  ${}^3\text{He-B}$  [27]. Shown here are the elements of the energy gap matrix  $\Delta$ , such that  $\mathbf{A} = e^{i\phi} \mathbf{R} \Delta$ . When the domain wall is absent  $\Delta$  is diagonal, see Eq. (1). Crossing the domain wall lying in  $yz$ -plane at  $x = 0$ ,  $\Delta_{zz}$  changes from  $\Delta_{\perp}$  to  $-\Delta_{\perp}$ , and off-diagonal elements  $\Delta_{xz}$  and  $\Delta_{zx}$  emerge, while  $\Delta_{xx}$  and  $\Delta_{yy}$  (not shown) remain close to  $\Delta_{\parallel}$ . The gap amplitudes were calculated  $z = 2.5\xi_0$  away from one of the surfaces in a  $D = 10\xi_0$  thick slab at  $T = 0.5T_c^{\text{bulk}}$ ;  $\xi_0$  is the Cooper pair diameter,  $\Delta_{\text{bulk}}$  is the bulk B phase gap.

pressure  $P = 0.03$  bar, where the bulk superfluid transition temperature  $T_c^{\text{bulk}} = 0.93$  mK, and close to specular scattering, achieved by preplating the cell walls with a  $64 \mu\text{mol}/\text{m}^2$  ( $\sim 5$  atomic layers)  ${}^4\text{He}$  film.

We first mapped the phase diagram with small tipping angle,  $\beta = 4^\circ$ , NMR pulses, Fig. 2a. The A-B transition was observed at  $T_{\text{AB}} = 0.7T_c^{\text{bulk}}$  in agreement with torsional oscillator measurements, with a  $1.08 \mu\text{m}$  cavity [33]. As we previously observed in the  $0.7 \mu\text{m}$  cavity, the B phase nucleated stochastically in two spin-orbit orientations with distinct NMR signatures: stable  $B_+$  and metastable  $B_-$  [32, 39].

The magnitudes of the frequency shifts of translationally invariant  $B_+$  and  $B_-$ ,  $\Delta f_+$  and  $\Delta f_-$ , are determined by averages of the gap structure across the cavity [32]:  $\langle \Delta_{\parallel}^2 \rangle$ ,  $\langle \Delta_{\parallel} \Delta_{\perp} \rangle$  and  $\langle \Delta_{\perp}^2 \rangle$ . In case of the putative spatially-modulated phase the averaging is also performed in the plane of the slab. This procedure is valid when the width of the stripes  $W$  is smaller than the dipole length  $\xi_D \approx 10 \mu\text{m}$  [32], a condition predicted to hold for this cavity ( $W \approx D\sqrt{3} \ll \xi_D$ ), except very close to the stripe-to-B transition [30]. In the stripe phase  $\langle \Delta_{\parallel} \Delta_{\perp} \rangle = 0$  due to  $\Delta_{\perp}$  having opposite sign in the adjacent domains [32]. This has clear signatures in the NMR response, as a function of tipping angle  $\beta$ .

We define the dimensionless gap distortion parameters

$$\bar{q} = \langle \Delta_{\parallel} \Delta_{\perp} \rangle / \langle \Delta_{\parallel}^2 \rangle, \quad \bar{Q} = \sqrt{\langle \Delta_{\perp}^2 \rangle / \langle \Delta_{\parallel}^2 \rangle}. \quad (2)$$

The tipping angle dependence of the frequency shift of  $B_+$ , below the so called “magic angle”,  $\beta^* > 104^\circ$ , scaled by the small-tipping-angle shift of  $B_-$  is given by [32]

$$\frac{\Delta f_+(\beta \rightarrow 0)}{\Delta f_-(\beta \rightarrow 0)} = \frac{2\bar{Q}^2 - \bar{q}^2 - 1}{1 + 2\bar{Q}^2}, \quad (3a)$$

$$\frac{\partial \Delta f_+(\beta) / \partial \cos \beta}{\Delta f_-(\beta \rightarrow 0)} = \frac{2\bar{Q}^2 - 2\bar{q}^2}{1 + 2\bar{Q}^2}, \quad (3b)$$

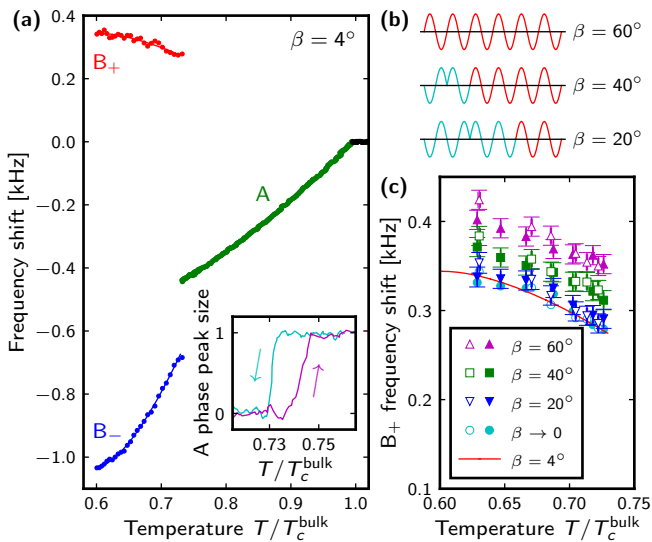


FIG. 2. NMR measurements on a  $D = 1.1 \mu\text{m}$  slab of superfluid  $^3\text{He}$ . (a) Signatures of the A and B phases observed with small tipping pulses. At the second-order normal-superfluid transition a negative frequency shift develops as the slab enters the A phase with the dipole-unlocked orientation. On further cooling a first-order phase transition into the B phase with a planar distortion occurs, where two spin-orbit orientations  $B_+$  and  $B_-$  are observed. Inset: sharp A-B transition with small hysteresis. (b) Technique for applying a set of pulses with different tipping angle  $\beta$  but equal heating: all pulses coincide in length and amplitude;  $\beta$  is reduced by applying the initial section of the pulse with a  $180^\circ$  phase shift, which cancels out a similar section that follows (both light blue), so only the remainder of the pulse (red) tips the spins. (c) Initial frequency shifts in  $B_+$  after such pulses yield  $\partial\Delta f_+/\partial\cos\beta$  and  $\Delta f_+(\beta \rightarrow 0)$ . Good agreement between  $\Delta f_+(\beta \rightarrow 0)$  obtained here and  $\Delta f_+(4^\circ)$ , smoothed from (a), indicates that the heating due to the  $20\text{-}60^\circ$  pulses is negligible. Open/filled symbols show data taken on step-wise warm-ups after a fast/slow cool-down from the A phase.

where  $\beta$  is the tip angle. We further note that:  $\Delta f_-(\beta)$  does not depend on  $\bar{q}$ ; the magic angle at which there is a kink in  $\Delta f_+(\beta)$  is given by  $\beta^* = \arccos(\bar{q} - 2)/(2\bar{q} + 2)$  [32]. Thus there is no magic angle expected for the stripe phase, for which  $\bar{q} = 0$ .

Application of large tipping pulses in our setup results in rapid heating of the confined helium via an unidentified mechanism, that previously restricted measurements of the planar distortion to temperatures well below  $T_{AB}$  [32, 40]. Here we focus on moderate pulses,  $\beta \lesssim 60^\circ$ , that allow us to probe the temperature dependence of the distortion parameters up to  $T_{AB}$ , according to Eq. (3). In order to measure the tipping-angle dependence of the frequency shift at constant temperature, we developed a scheme for applying pulses with different  $\beta$  while inducing identical heating, shown in Fig. 2b. Triplets of such pulses with  $\beta = 20^\circ$  to  $60^\circ$  were applied to  $B_+$  during step-wise warm-ups after a fast (at approx.  $40 \mu\text{K}/\text{min}$

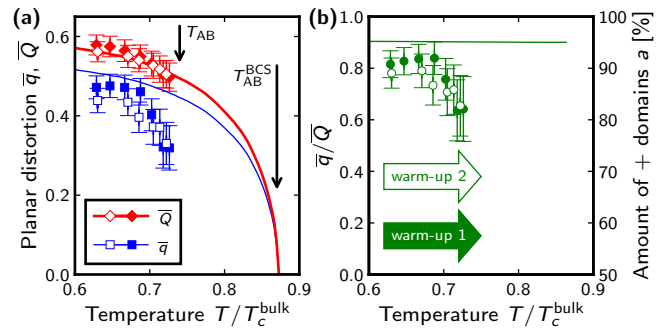


FIG. 3. Temperature dependence of planar distortion parameters  $\bar{q}$ ,  $Q$  (a) and their ratio (b) inferred from NMR measurements, Fig. 2. Solid lines show weak-coupling calculations for translationally-invariant B phase [44]. In the absence of strong coupling the temperature of the AB transition  $T_{AB}^{\text{BCS}}$  is higher than  $T_{AB}$  observed experimentally. While  $Q$  is in agreement with the theory,  $\bar{q}$  gets progressively reduced approaching  $T_{AB}$ . We interpret this in terms of development of domains with opposite sign of  $\Delta_\perp$  on warming. The right-hand vertical axis in (b) estimates the fraction of the slab occupied by the majority domains, taken here to have positive  $\Delta_\perp$  [45], under a qualitative assumption of step-like energy gap profile, Eq. (4). Any systematic difference between measurements taken while warming after a fast and a slow cool-down through A-B transition (open/filled symbols) is small.

rate) and slow ( $4 \mu\text{K}/\text{min}$ ) cool-down through the A-B transition. We inferred  $\partial\Delta f_+/\partial\cos\beta$  and  $\Delta f_+(\beta \rightarrow 0)$  from the data shown in Fig. 2c and confirmed the heating effects to be negligible for the chosen pulses. Combining with  $\Delta f_-(4^\circ)$  at the same temperature, Fig. 2a, we determine the planar distortion parameters  $\bar{q}$  and  $Q$  through Eq. (3), shown in Fig. 3.

In the above analysis the off-diagonal elements of the gap matrix near domain walls (see Fig. 1) have been neglected. Incorporating the detailed gap structure at the domain walls into the NMR model leaves the signature of the stripe phase,  $\bar{q} = 0, Q > 0$ , virtually unchanged [30]. We can therefore conclude unambiguously that the stripe phase was not present in our experiment.

Nevertheless, while  $Q$  matches the weak-coupling calculations for the translationally-invariant B phase [44],  $\bar{q}$  is found to be reduced, see Fig. 3. This contrasts with the good agreement between these calculations and similar measurements in a  $D = 0.7 \mu\text{m}$  slab at higher pressure [32, 40], ruling out strong coupling effects as the origin of this discrepancy. We therefore consider domain structures in which the amount  $a$  and  $1 - a$  of domains with positive and negative  $\Delta_\perp$  is unequal [45]. For a qualitative estimate we assume that the domain walls are step-like and ignore gap variation across the slab,  $\Delta_\parallel = \text{const}, |\Delta_\perp| = \text{const}$ . Then

$$\bar{Q} = \frac{|\Delta_\perp|}{\Delta_\parallel}, \quad \bar{q} = (2a - 1) \frac{|\Delta_\perp|}{\Delta_\parallel}, \quad \frac{\bar{q}}{Q} = 2a - 1, \quad (4)$$

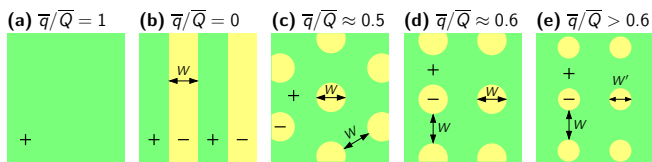


FIG. 4. Possible regular domain configurations in  $^3\text{He-B}$  confined to a slab, view perpendicular to the slab plane.  $+/-$  indicates the sign of  $\Delta_{\perp}$ . (a) Translationally-invariant B phase, (b) predicted stripe phase, (c,d) proposed polka dot phase that is easier to nucleate than the stripe phase. The values of the gap distortion parameter  $\bar{q}/\bar{Q}$  are derived under a simplified assumption of step-like domain walls, Eq. (4). Pinning of domain walls in the experimental cell may introduce disorder to these structures. All features in (c-d) are taken to be of characteristic size similar to the pitch  $W$  of the stripe phase. (e) A variant of (d) in which dot diameter  $W'$  is smaller than dot separation  $W$ .

demonstrating that while  $\bar{q}$  is sensitive to the presence of domains, to the first approximation  $\bar{Q}$  is not, in agreement with our observations. The gradual variation of  $\Delta_{\parallel}$ ,  $\Delta_{\perp}$  and the emergence of the off-diagonal gap matrix elements inside the domain walls would lead to corrections to this model that should be taken into account in future theoretical work.

Our measurement  $\bar{q}/\bar{Q} = 0.6 \pm 0.1$  near  $T_{AB}$  suggests a  $+/-$  domain proportion of 4 : 1. A likely scenario for an imbalance of the domains is a two-dimensional structure. Within possible regular morphologies, Fig. 4, this imbalance corresponds to a *polka dot phase* with hexagonal or square symmetry, Fig. 4c,d. Such structures have been suggested theoretically [27], but the detailed analysis of their energetic stability has not been carried out. A preliminary Ginzburg-Landau study finds the square lattice of dots, Fig. 4d, to be locally stable, with free energy only slightly higher than that of the stripe phase [46]. Further theoretical work is required to understand the stability of various modulated states in the presence of strong coupling effects.

Even if less energetically favourable than stripes, the dots may arise because of a lower energy barrier for flipping the sign of  $\Delta_{\perp}$  in a microscopic dot, compared with a stripe, that is macroscopic in one dimension. A lattice of dots would form if the neighbouring dots nucleate close enough to prevent them from growing beyond a typical size  $W$  before getting within  $W$  of the others.

Our experimental protocol is first to cool deep into the B phase, in order to destabilise the domain walls, and then to take data on warming. The key observation of the decrease in  $\bar{q}/\bar{Q}$  with increasing temperature is consistent with the formation of negative-energy domain walls in the B phase approaching the transition into the A phase, as predicted theoretically. The observation of a single NMR line implies that the domain size is shorter than  $\xi_D$ . The measured temperature dependence of  $\bar{q}/\bar{Q}$  can

be explained by allowing the separation between dots  $W$  and their diameter  $W'$  be unequal, see Fig. 4e. Pinning of the domain walls by scratches on the cavity walls [47] may play a role in restricting  $W'$ , and introduce disorder into the domain morphology. Improved cavities have been developed for future experiments [48].

As an alternative scenario, we now consider metastable domain walls with positive energy. Defects are known to form at the A-B transition either due to inhomogeneous nucleation [49, 50] or as relics [51] of defects, present in the A phase at the start of the transition [52, 53]. These may include the domain walls where  $\Delta_{\perp}$  changes sign [29, 51, 54, 55], which, if produced at unusually high density, would result in a reduced  $\bar{q}/\bar{Q}$  ratio; however this ratio would remain constant if the defects are pinned or increase with time as they decay, contrary to our observation. This does not rule out sparse positive-energy defects with typical separation larger than  $\xi_D$ , giving rise to small satellite NMR signals, specific to each type of defect [51, 53, 56, 57]. Detection of such signals is beyond the scope of this work. Within errors our observations are independent of the rate of cooling through the A-B transition, Fig. 3. This supports our proposal that defects produced at this transition do not play a major role in the formation of domains on micron scale. A systematic study of the influence of the cooling rate will be subject of future work.

In conclusion our NMR study of superfluid  $^3\text{He}$  confined in a  $1.1\ \mu\text{m}$  cavity in the vicinity of the AB transition has found neither the predicted stripe phase, nor translationally-invariant planar-distorted B phase. This leads us to propose a superfluid phase with two-dimensional spatial modulation, in a form of a regular or disordered array of island domains, driven by negative energy of domain walls under confinement. Further systematic studies of the nucleation of this phase, to determine the equilibrium morphology, as well as its stability as a function of pressure, predicted to be influenced by strong coupling effects, are both desirable. Superfluid  $^3\text{He}$  under confinement appears to provide a clean model system for spatially modulated superconductivity/superfluidity, long sought in a wide variety of physical systems.

We thank B. R. Ilic for help with microfluidic chamber fabrication and design methodology; A. B. Vorontsov and J. A. Sauls for sharing calculations of the gap profile of confined  $^3\text{He}$ ; T. Kawakami and T. Mizushima for a stimulating discussion and for sharing their preliminary result on the stability of the polka dot phase. This work was supported by EPSRC grants EP/J022004/1 and EP/R04533X/1; NSF grants DMR-1202991 and DMR-1708341, and the European Microkelvin Platform.

\* l.v.levitin@rhul.ac.uk

- <sup>†</sup> Now at Institute for Quantum Computing, University of Waterloo, Waterloo, Ontario N2L 3G1, Canada
- <sup>‡</sup> Now at Imperial College London, London SW7 2AZ, UK
- <sup>§</sup> Now at Corning Incorporated, USA
- <sup>¶</sup> Now at Vantage Power Ltd, London, UB6 0FD, UK
- [1] J. Bardeen, L. N. Cooper and J. R. Schrieffer, *Phys. Rev.* **108**, 1175 (1957).
- [2] L. N. Cooper, *BCS: 50 years* (World Scientific, 2011).
- [3] G. R. Stewart, *Adv. in Phys.* **66**, 75 (2017).
- [4] A. J. Leggett, *Rev. Mod. Phys.* **47**, 332 (1975).
- [5] D. Vollhardt and P. Wolfe, *The superfluid phases of <sup>3</sup>He* (Taylor and Francis, 1990).
- [6] S. Giorgini, L. P. Pitaevskii, and S. Stringari, *Rev. Mod. Phys.* **80**, 1215 (2008).
- [7] A. B. Migdal, *Nucl. Phys.* **13**, 655 (1959).
- [8] A. A. Abrikosov, *Sov. Phys.-JETP*, **5**, 6, 1174 (1957).
- [9] A. I. Larkin and Yu. N. Ovchinnikov, *Sov. Phys. JETP* **20**, 762 (1965).
- [10] P. Fulde and R. A. Ferrell, *Phys. Rev. A* **135**, 550 (1964).
- [11] Y. Matsuda and H. Shimahara, *J. Phys. Soc. Jpn* **76**, 051005 (2007).
- [12] J. Wosnitza, *Ann. Phys. (Berlin)* **530**, 1700282 (2018).
- [13] H. Mayaffre, S. Krämer, M. Horvatić, C. Berthier, K. Miyagawa, K. Kanoda, and V. F. Mitrović, *Nat. Phys.* **10**, 928 (2014).
- [14] C. C. Agosta, N. A. Fortune, S. T. Hannahs, S. Gu, L. Liang, J.-H. Park, and J. A. Schlueter, *Phys. Rev. Lett.* **118**, 267001 (2017).
- [15] R. Beyer, B. Bergk, S. Yasin, J. A. Schlueter, and J. Wosnitza, *Phys. Rev. Lett.* **109**, 027003 (2012).
- [16] G. Koutroulakis, H. Kühne, J. A. Schlueter, J. Wosnitza, and S. E. Brown, *Phys. Rev. Lett.* **116**, 067003 (2016).
- [17] Sh. Kitagawa, G. Nakamine, K. Ishida, H. S. Jeevan, C. Geibel, and F. Steglich, *Phys. Rev. Lett.* **121**, 157004 (2018).
- [18] A. Bianchi, R. Movshovich, C. Capan, P. G. Pagliuso, and J. L. Sarrao, *Phys. Rev. Lett.* **91**, 187004 (2003).
- [19] G. Koutroulakis, M. D. Stewart, Jr., V. F. Mitrović, M. Horvatić, C. Berthier, G. Lapertot, and J. Flouquet, *Phys. Rev. Lett.* **104**, 087001 (2010).
- [20] D. Y. Kim, S.-Z. Lin, F. Weickert, M. Kenzelmann, E. D. Bauer, F. Ronning, J. D. Thompson, and R. Movshovich, *Phys. Rev. X* **6**, 041059 (2016).
- [21] D. Y. Kim, S.-Z. Lin, F. Weickert, E. D. Bauer, F. Ronning, J. D. Thompson, and R. Movshovich, *Phys. Rev. Lett.* **118**, 197001 (2017).
- [22] M. H. Hamidian, S. D. Edkins, S. H. Joo, A. Kostin, H. Eisaki, S. Uchida, M.J. Lawler, E.-A. Kim, A.P. Mackenzie, K. Fujita, J. Lee, and J. C. Séamus Davis, *Nature* **532**, 343 (2016).
- [23] M. W. Zwierlein, A. Schirotzek, C. H. Schunck, and W. Ketterle, *Science*, **311**, 492 (2006).
- [24] M. C. Revell, J. A. Fry, B. A. Olsen, and R. G. Hulet, *Phys. Rev. Lett.* **117**, 235301 (2016).
- [25] R. Casalbuoni and G. Nardulli, *Rev. Mod. Phys.* **76**, 263 (2004).
- [26] S. Dutta and E. J. Mueller, *Phys. Rev. A* **96**, 023612 (2017).
- [27] A. B. Vorontsov and J. A. Sauls, *Phys. Rev. Lett.* **98**, 045301 (2007), *J. Low Temp. Phys.* **138**, 283 (2005).
- [28] M.M. Salomaa and G.E. Volovik, *Phys. Rev. B* **37**, 9298 (1988).
- [29] M. Silveri, T. Turunen, and E. Thuneberg, *Phys. Rev. B* **90**, 184513 (2014).
- [30] J. J. Wiman and J. A. Sauls, *J. Low Temp. Phys.* **184**, 1054 (2016).
- [31] K. Aoyama, *J. Phys. Soc. Jpn.* **85**, 094604 (2016).
- [32] L. V. Levitin, R. G. Bennett, E. V. Surovtsev, J. M. Parpia, B. Cowan, A. J. Casey, J. Saunders, *Phys. Rev. Lett.* **111**, 235304 (2013).
- [33] N. Zhelev, T. S. Abhilash, E. N. Smith, R. G. Bennett, X. Rojas, L. Levitin, J. Saunders, and J. M. Parpia, *Nat. Comm.* **8**, 15963 (2017).
- [34] Y. Nagato and K. Nagai, *Physica B* **284-288**, 269 (2000).
- [35] Note that the state with  $\Delta_{\perp} < 0$  on the right of the domain wall in Fig. 1 can be written in the canonical form Eq. (1) with  $\Delta_{\perp} > 0$  using a  $\pi$  phase shift and a combined rotation  $\mathbf{R}(\hat{\mathbf{n}}', \theta') = \mathbf{R}(\hat{\mathbf{n}}, \theta)\mathbf{R}(\hat{\mathbf{z}}, \pi)$ :
- $$e^{i\phi}\mathbf{R}(\hat{\mathbf{n}}, \theta) \begin{pmatrix} \Delta_{\parallel} & & \\ & \Delta_{\parallel} & \\ & & -\Delta_{\perp} \end{pmatrix} = -e^{i\phi}\mathbf{R}(\hat{\mathbf{n}}, \theta) \begin{pmatrix} -\Delta_{\parallel} & & \\ & -\Delta_{\parallel} & \\ & & \Delta_{\perp} \end{pmatrix} \\ = e^{i(\phi+\pi)}\mathbf{R}(\hat{\mathbf{n}}, \theta)\mathbf{R}(\hat{\mathbf{z}}, \pi) \begin{pmatrix} \Delta_{\parallel} & & \\ & \Delta_{\parallel} & \\ & & \Delta_{\perp} \end{pmatrix}.$$
- [36] K. Aoyama, *Phys. Rev. B* **89**, 140502R (2014).
- [37] J. J. Wiman and J. A. Sauls, arXiv:1802.08719 (2018).
- [38] A. B. Vorontsov, *Phys. Rev. Lett.* **102**, 177001 (2009).
- [39] L. V. Levitin, R. G. Bennett, A. Casey, B. Cowan, J. Saunders, D. Drung, Th. Schurig, and J. M. Parpia, *Science* **340**, 841 (2013).
- [40] See Supplemental Material at [URL will be inserted by publisher] for details of the experimental setup, NMR, thermometry, comparison of the measured  $\bar{q}$  and  $\bar{Q}$  to Ref. [32], and qualitative comparison of domain configurations. This includes Refs. [41–43].
- [41] L. V. Levitin, R. G. Bennett, A. Casey, B. Cowan, J. Saunders, D. Drung, Th. Schurig, J. M. Parpia, B. Ilic, and N. Zhelev, *J. Low Temp. Phys.* **75**, 667 (2014).
- [42] V. Dotsenko and N. Mulders. *J. Low Temp. Phys.* **134**, 443 (2004).
- [43] P. J. Heikkinen, A. Casey, L. V. Levitin, X. Rojas, A. Vorontsov, N. Zhelev, J. M. Parpia, and J. Saunders, *Tuning pair-breaking at the surface of topological superfluid <sup>3</sup>He* (unpublished).
- [44] A. B. Vorontsov and J. A. Sauls, *Phys. Rev. B* **68**, 064508 (2003) and private communication.
- [45] Since the sign of  $\Delta_{\perp}$  can be flipped throughout the sample with a uniform transformation [35], we only need to consider the case of  $\Delta_{\perp}$  being positive in the larger part of the slab,  $a \geq 0.5$ , so  $\bar{q} \geq 0$ , as required in Eq. (3) [32].
- [46] T. Kawakami and T. Mizushima, private communication (2018).
- [47] Analogous to weak pinning of the A-B boundary observed in the similarly fabricated  $D = 0.7 \mu\text{m}$  cavity [39].
- [48] N. Zhelev, T. S. Abhilash, R. G. Bennett, E. N. Smith, B. Ilic, J. M. Parpia, L. V. Levitin, X. Rojas, A. Casey, and J. Saunders, *Rev. Sci. Instr.* **89**, 073902 (2018).
- [49] D. I. Bradley, S. N. Fisher, A. M. Guénault, R. P. Haley, J. Kopu, H. Martin, G. R. Pickett, J. E. Roberts, and V. Tsepelin, *Nat. Phys.* **4**, 46 (2008).
- [50] P. J. Heikkinen, S. Autti, V. B. Eltsov, R. P. Haley, and V. V. Zavjalov, *J. Low Temp. Phys.* **175**, 681 (2014).
- [51] J. T. Mäkinen, V. V. Dmitriev, J. Nissinen, J. Rysti, G. E. Volovik, A. N. Yudin, K. Zhang, V. B. Eltsov, arXiv:1807.04328v3.



- [52] P. M. Walmsley and A. I. Golov, Phys. Rev. Lett. **109**, 215301 (2012).  
 [53] J. Kasai, Y. Okamoto, K. Nishioka, T. Takagi, and Y. Sasaki, Phys. Rev. Lett. **120**, 205301 (2018).  
 [54] Yu. Mukharsky, O. Avenel, and E. Varoquaux, Phys. Rev. Lett. **92**, 210402 (2004).  
 [55] C. B. Winkelmann, J. Elbs, Yu. M. Bunkov, and H. Godfrin, Phys. Rev. Lett. **96**, 205301 (2006).

- [56] V. B. Eltsov, R. Blaauwgeers, N. B. Kopnin, M. Krusius, J. J. Ruohio, R. Schanen, and E. V. Thuneberg, Phys. Rev. Lett. **88**, 065301 (2002).  
 [57] S. Autti, V. V. Dmitriev, J. T. Mäkinen, A. A. Soldatov, G. E. Volovik, A. N. Yudin, V. V. Zavjalov, and V. B. Eltsov, Phys. Rev. Lett. **117**, 255301 (2016).

## Supplemental Material

### EXPERIMENTAL SETUP

The apparatus of this experiment is in most aspects identical to that used in Ref. [39] and described in its supplementary material. The main difference is the improved uniformity of the cavity, see Fig. S1, achieved through optimised nanofabrication, introduction of a partition wall and restricting the measurements to low pressure [41]. In addition the cell fill line was interrupted with a superfluid-leaktight cryogenic valve [41, 42] at 6 mK, to avoid gradual depletion of the  $^4\text{He}$  film due to the fountain effect.

### TEMPERATURE CORRECTION

The thermometry in our experimental setup is based on monitoring the temperature of the silver sinter heat

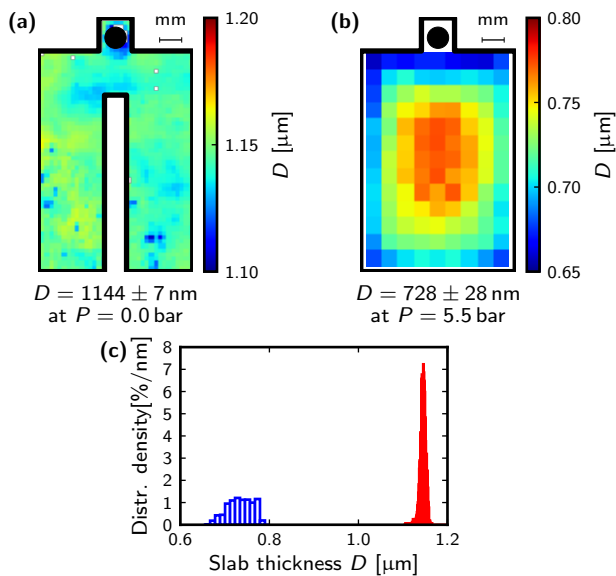


FIG. S1. Spectroscopic measurement of the thickness  $D$  of silicon-glass microfluidic cavities. The  $1.1 \mu\text{m}$  cavity used in the experiment described here is compared to the  $0.7 \mu\text{m}$  cavity from Refs. [32, 39], inflated under pressure necessary to stabilise the B phase. In the present work the slab uniformity is improved, one of the reasons being the partition wall in the middle of the cell [41].

exchanger with a  $^{195}\text{Pt}$  NMR thermometer, calibrated against the  $^3\text{He}$  melting curve. In recent work on a  $D = 0.2 \mu\text{m}$  slab [43] the temperature gradient between silver sinter (at  $T_{\text{Ag}}$ ) and helium (at  $T_{\text{He}}$ ) in the heat exchanger was carefully determined for various surface  $^4\text{He}$  coverages. With  $^4\text{He}$  plating similar to the one used in this experiment, the correction was found to be

$$T_{\text{He}}^{3.5} - T_{\text{Ag}}^{3.5} = C, \quad (\text{S1})$$

corresponding to thermal boundary resistance  $R_{\text{K}}(T) \propto 1/T^{2.5}$ . The constant  $C$  in (S1), determined by heat leak

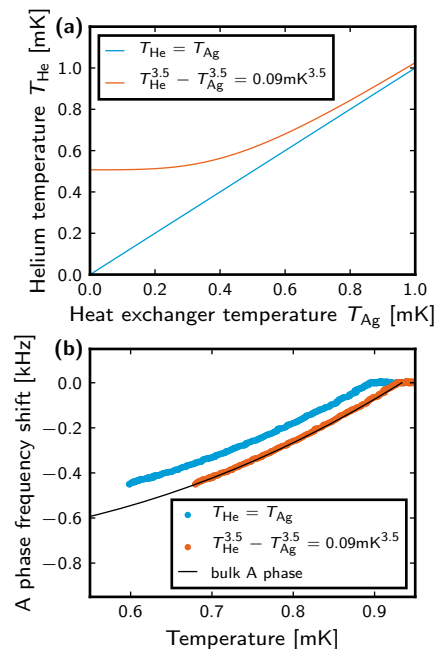


FIG. S2. Temperature correction. (a) Relationship between temperatures  $T_{\text{He}}$  and  $T_{\text{Ag}}$  of helium and silver sinter in the heat exchanger. (b) Frequency shift in the A phase is expected to have the bulk value, since the energy gap in the A phase is not suppressed in a slab with specular walls. This is found to be the case after the temperature correction. Here the bulk frequency shift is modelled based on the initial slope  $2f_L \partial |\Delta f(T)| / \partial (1 - T/T_c)|_{T \rightarrow T_c} = 3.96 \times 10^9 \text{ Hz}^2$  measured in the  $D = 0.2 \mu\text{m}$  cavity with 98%-specularly scattering walls and the calculated temperature dependence of the weak-coupling A phase energy gap. Here the initial slope is defined as the slope of a straight line fitted between  $0.9T_c$  and  $1.0T_c$ .

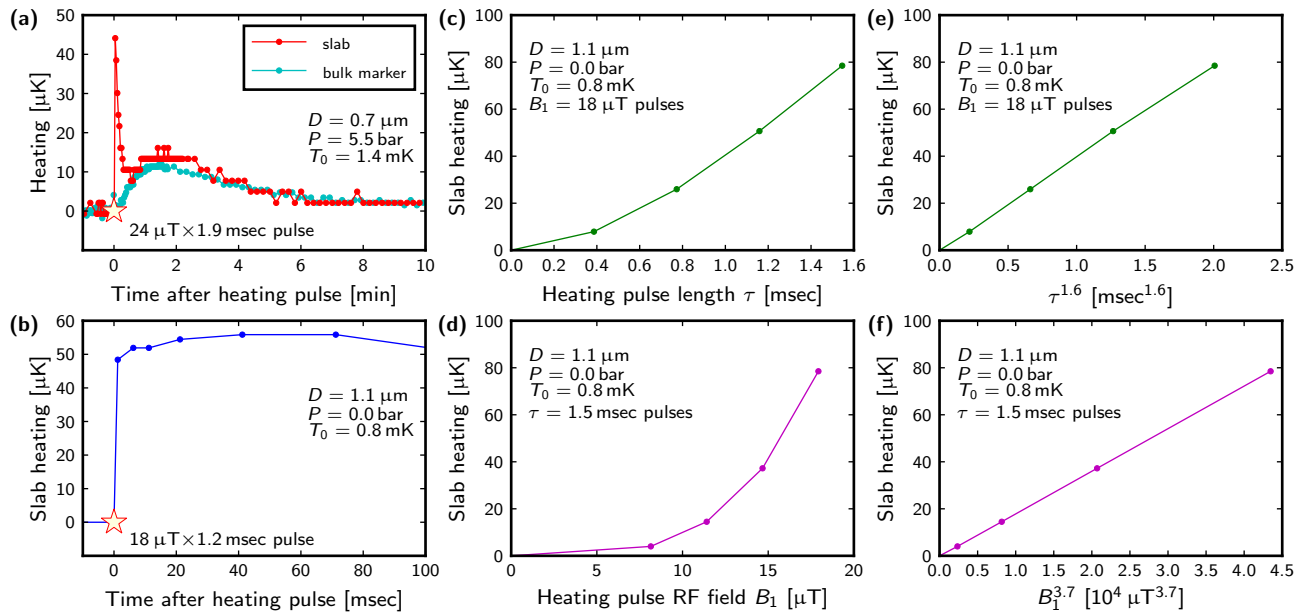


FIG. S3. Characterisation of heating of the confined  $^3\text{He}$  by NMR pulses. Helium temperature is inferred from frequency shift probed regularly with small NMR pulses, while the heating is induced by large pulses, applied sufficiently far from Larmor frequency not to tip  $^3\text{He}$  spins and rarely enough (once every 20 minutes) to let the sample cool down before it is heated again. (a) Heating in the slab and the “bulk marker” volume at the mouth of the fill line. Only the former rapidly warms up due to local heating we are concerned with; in addition both slowly respond to Joule heating of the metallic elements of the experimental setup, transmitted via the heat exchanger. Data from the  $D = 0.7 \mu\text{m}$  slab with a large clearly-visible bulk marker [39]. The rest of the measurements were performed on the  $D = 1.1 \mu\text{m}$  slab presented in this paper. (b) Time evolution of the slab temperature shortly after a large pulse. (c-f) Dependence of heating on the pulse duration  $\tau$  and power of radio-frequency field  $B_1$  measured 20 msec after pulses, when the slab reaches its highest temperature.

to the helium sample, is obtained from the suppression of bulk  $T_c$ , registered with NMR in the bulk  $^3\text{He}$  marker at the mouth of the fill line. Fig. S2 demonstrates that such correction with a slightly different  $C$  is adequate for the present experiment, which utilised the same heat exchanger. In this work the NMR pulses were applied rarely enough to have no effect on  $C$ .

### HEATING BY NMR PULSES

NMR experiments on superfluid  $^3\text{He}$  under regular confinement in silicon-glass and fully-silicon cavities (Refs. [32, 39, 43] and this work) have manifested heating of an unidentified origin that couples to the confined liquid directly, Fig. S3a. Most heating occurs within 1 msec after the pulse (the duration of the probe NMR pulse plus the dead time of the NMR spectrometer), and the slab temperature is nearly constant for many msec afterwards, Fig. S3b. The dependence of the heating on duration  $\tau$  and amplitude  $B_1$  of the sine-wave pulses, Fig. S3c-f, is steeper than expected for linear dissipation ( $Q \propto \tau B_1^2$ ), especially when taking into account that specific heat of  $^3\text{He}$  in the slab increases with temperature. This points towards an exotic origin of this parasitic effect.

In addition to the signatures shown in Fig. S3 we found

that the heating is not resonant near the  $^3\text{He}$  Larmor frequency, and that heating due to pulses with the initial ‘antipulse’, Fig. 2b, only depends on the total duration and amplitude, but not on the length of the ‘antipulse’ part.

As shown in Fig. S3b, the free induction decay after a large pulse with characteristic  $T_2^* \approx 3\text{-}10 \text{ msec}$  occurs at a nearly constant temperature, elevated above the

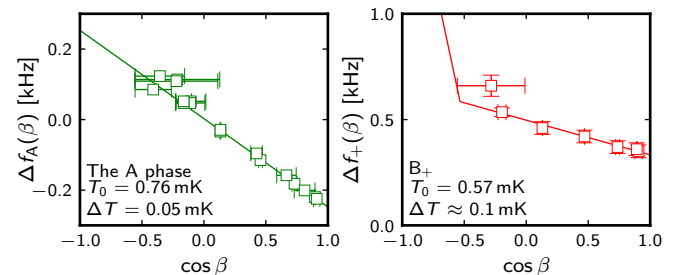


FIG. S4. NMR measurements on the A and B phase in  $D = 1.1 \mu\text{m}$  slab with  $18 \mu\text{T} \times 1.2 \text{ msec}$  pulses. These pulses overheated the slab by  $\Delta T$  above the temperature  $T_0$  of the helium in the heat exchanger. Different tipping angles are achieved by applying the initial part of the pulse with a  $180^\circ$  phase shift, see Fig. 2b. In the dipole-unlocked A phase  $\Delta f_A(\beta) \propto \cos \beta$ , see [32] for  $\Delta f_+(\beta)$ .

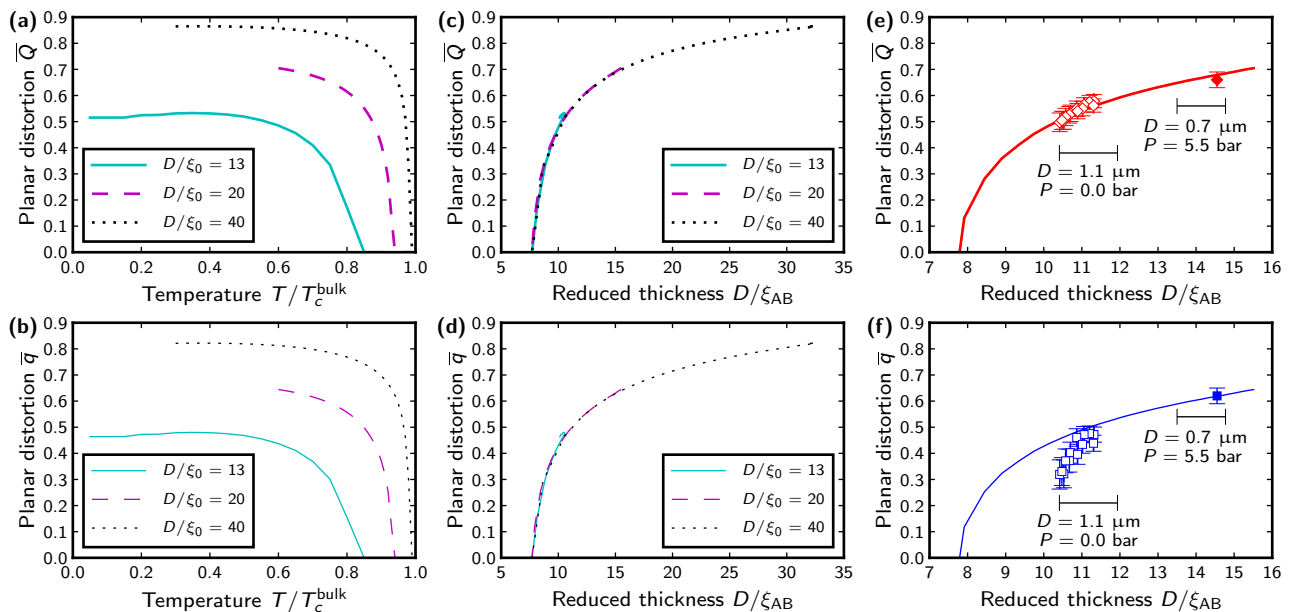


FIG. S5. Universal scaling of planar distortion parameters  $\bar{q}$  and  $\bar{Q}$  with reduced slab thickness  $D/\xi_{AB}$ . (a-d) Calculations of planar distortion of spatially-invariant planar-distorted B phase at various  $D/\xi_0$  [44]. See Eq. (S3) for the definition of the coherence length. (e-f) Comparison of these calculations to measurements on 0.7  $\mu\text{m}$  slab (filled symbols) [32] and 1.1  $\mu\text{m}$  slab (open symbols, showing together both warm-ups presented in Fig. 3). The horizontal bars represent the range of  $D/\xi_{AB}$  that can be probed in at given  $D$  and  $P$  limited by  $T = T_{AB}$  and  $T = 0$ .

temperature  $T_0$  of helium in the heat exchanger and fill line. The use of ‘antipulses’, Fig. 2b, allows us to measure the NMR response as a function of tipping angle at a *constant* elevated temperature. This is illustrated in Fig. S4. We note that the strong frequency dependence of NMR tipping by ‘antipulses’, renders them unusable away from their carrier frequency. For this reason  $B_-$  is missing from Fig. S4, due to relatively large frequency range spanned by  $\Delta f_-(\beta) \approx -1 \text{ kHz} \times \cos(\beta)$ . Probing  $B_+$  above the magic angle  $\beta^*$  is equally problematic and was not studied here in detail.

In contrast the 0.7  $\mu\text{m}$  slab was probed with groups of large pulses that caused different heating, restricting such measurements to the  $T \lesssim 0.5T_c$  limit where the temperature dependence of the frequency shifts is weak [32].

In this work we demonstrated that tipping angles up to  $60^\circ$  could be reached with  $8 \mu\text{T} \times 1.2 \text{ msec}$  pulses, generating only  $\Delta T \lesssim 10 \mu\text{K}$ , small compared to the temperature range over which we probed the B phase gap distortion.

### UNIVERSAL SCALING OF PLANAR DISTORTION

Within the Ginzburg-Landau regime,  $T - T_c \ll T_c$ , the effects of confinement on properties of the superfluid are determined by a single control parameter, the reduced thickness  $D/\xi(T, P)$ , where  $\xi$  is the coherence

length. This universality breaks down at lower temperatures, i.e. see the supplementary of Ref. [39]. To study the A-B transition outside of the Ginzburg-Landau regime the coherence length has been defined as

$$\xi_\Delta(T, P) = \frac{\hbar v_F(P)}{\Delta_B(T, P)\sqrt{10}}, \quad (\text{S2})$$

where  $v_F$  is the Fermi velocity and  $\Delta_B$  is the bulk B phase gap. We observe that the weak-coupling quasiclassical calculations [44] of  $\bar{q}(T)$  and  $\bar{Q}(T)$  at different  $D$  collapse, see Fig. S5a-d, expressed as a function of  $D/\xi$  adopting a slightly different coherence length

$$\xi_{AB}(T, P) = \frac{D_{AB}(T, P)}{\pi\sqrt{6}}, \quad (\text{S3})$$

where  $D_{AB}(T, P)$  is the thickness of the slab at which the A to B transition occurs at temperature  $T$  and pressure  $P$  (the inverse of the  $T_{AB}(D/\xi_0(P))$  function [34]). Here we restrict the discussion to the calculations for a slab with specular boundaries and recognise that the pressure  $P$  only enters the weak-coupling calculations via the pressure dependence of the bulk transition temperature  $T_c^{\text{bulk}}(P)$  and the Cooper pair diameter  $\xi_0(P) = \hbar v_F(P)/2\pi k_B T_c^{\text{bulk}}(P)$ . We find that  $\xi_{AB}/\xi_\Delta \rightarrow 1.0$  at  $T \rightarrow T_c$  and  $\xi_{AB}/\xi_\Delta \rightarrow 1.1$  at  $T \rightarrow 0$ .



## PLANAR DISTORTION: THEORY VS EXPERIMENTS

We compare the calculations discussed in the previous section with the NMR measurements of the planar distortion of the B phase in 0.7 and 1.1  $\mu\text{m}$  slabs in Fig. S5e,f. The former, obtained at  $P = 5.5$  bar and  $T = 0.6$  mK  $= 0.4T_c^{\text{bulk}}$  are in good agreement with the theory in terms of both  $\bar{q}$  and  $\bar{Q}$ . This confirms that the strong coupling effects, known to increase with pressure, are not responsible for the reduced  $\bar{q}$  presented in this paper, Fig. 3 and Fig. S5f.

## QUALITATIVE DISCUSSION OF DOMAIN CONFIGURATIONS

In this section we compare possible structures of domains using the length of domain walls per unit area of the slab  $L/A$  as a figure of merit of the free energy gain due to formation of domain walls. We consider a two-dimensional problem of energetic stability of thin domain walls with hard-core repulsion at distance  $W$ . Dots are assumed to be circular. We find  $L/A = 1/W$  for the stripe phase,  $L/A = \pi/2W\sqrt{3} \approx 0.91/W$  for hexagonal lattice and  $L/A = \pi/4W \approx 0.79/W$  for square lattice, listed in Fig. 4b-d. The fact that these numbers are all close to each other demonstrates that the free energy of 1D and 2D modulated states is nearly degenerate, and only a detailed calculation can reliably identify the lowest energy state, taking into account the gradual spatial variation of the order parameter components across the domain walls and the optimum shape of dots.